Makarov *et al. ROBOMECH Journal* (2023) 10:19
https://doi.org/10.1186/s40648-023-00259-7

ROBOMECH Journal

RESEARCH ARTICLE

Open Access

Implementation of interactive control of a crane ship model in MATLAB/Simulink environment

Oleg Makarov[1*], Hayato Yase[2] and Takashi Harada[2]

Abstract

The increased demand for performing crane ship modeling has led to the necessity for fast and accurate numerical experiments. This paper presents an approach for creating a numerical model of a crane vessel with a suspended load that allows for real-time control of crane parts. The model is developed in the MATLAB/Simulink environment, which makes it possible to extend it further to the user's needs. The authors describe the approach to the calculation of wave-induced ship motions, presents the Simulink block model and describes the features encountered during the simulation process. The possibility of real-time control of the position of crane parts is also shown, keeping the calculation speed of the ship hydrodynamics.

Keywords Marine construction, Crane vessel, Interactive simulation, Multibody dynamics, Numerical simulation, Offshore operations

Introduction

Crane ships are the type of offshore support vessels (OSV) that perform marine construction operations. These vessels are impacted by natural forces such as waves, wind, and currents, making such operations more complex than their land-based counterparts. The complexity of the analysis of such facilities is an order of magnitude higher than for onshore cranes, which can be modeled using only multibody dynamics (MBD). If the laws of dynamics are well studied and represented by ordinary differential equations, such as Newton's equations of motion, then in the case of floating cranes the critical point here is the transition to the field of hydrodynamics.

*Correspondence:
Oleg Makarov
dadidal96@gmail.com
[1] Graduate School of Science and Engineering, Kindai University, 3-4-1 Kowakae, Higashiosaka, Osaka 577-8502, Japan
[2] Faculty of Science and Engineering, Kindai University, 3-4-1 Kowakae, Higashiosaka, Osaka 577-8502, Japan

The determination of hydrodynamic forces is still a challenging task due to the features of the fluid medium, such as viscosity and turbulence. Computational fluid dynamics (CFD) methods are used and received wide development to solve such problems.

The most accurate result can be obtained by applying a CFD method based on the well-known Navier–Stokes partial differential equations, taking into account flow turbulence and fluid viscosity. Such numerical models provide the most comprehensive insight into the dynamics of a floating object, but the computational cost of such calculations is extremely high. For example, Wang et al. [1] performed CFD simulations of free-decay tests to determine the damping coefficients of a floating structure. The simulation time for a 20-s case was up to 44.4 h. Considering the necessity to calculate different states and directions of waves, wind, and other factors, such studies turn into very time-consuming and labor-intensive numerical experiments. Therefore, the implementation of MBD and CFD co-simulation in the time domain using this approach or the so-called two-way coupling did not find wide application in real practice.

For real-world engineering applications, co-simulation with one-way coupling is used, in which CFD and MBD calculations are performed separately and consecutively. In this case, first, one-time CFD calculations in the frequency domain are performed to determine the frequency-dependent hydrodynamic coefficients. The potential flow theory is used for this purpose, which makes it possible to consider multiple states (frequencies and directions) of the sea. Afterward, these coefficients are used in the time domain to determine the hydrodynamic forces as external forces in the MBD solver. For instance, this approach was used by Cha et al. [2] and Hong et al. [3] to simulate the dynamic response of a crane ship with a suspended load.

At the current stage of software development, there is no need to develop solvers from scratch. MBD has a simpler algorithm than CFD and it is possible to develop in-house software, while the graphical interface can be created using external libraries. As for CFD, there are many commercial and open-source tools for this kind of numerical analysis. For coupled multiphysics analysis, some authors linked CFD and MBD through their own developed application programming interfaces (APIs). Viswanathan et al. [4] demonstrated an approach for modeling the lifting and lowering of cargo by a crane ship using the Modelica-based simulation package SimulationX and the CFD solver OrcaFlex. The simulation of 260-s event took approximately 1 h.

The mentioned multiphysics co-simulation approach showed reasonable results but has obvious drawbacks from a technical point of view. If the CFD and MBD solvers and the API are implemented in different programming languages, the obvious effect of this connection will be a slowdown in the computation speed. In addition, upgrading a version of one software cannot guarantee reliable functioning with an old version of another solver and may require an update of the API linking them. Therefore, to ensure the reliability and speed of calculations, minimizing the number of links between separate software is necessary.

As for the simultaneous CFD and MBD calculation in one program, there are several commercial and open-source numerical analysis programs available today as well. For instance, Cha et al. [5], Ha et al. [6] and Ku et al. [7] developed their own frameworks for modeling crane ship dynamics. In such programs, it is possible to consider various environmental forces and sea states. Also, they include the possibility of controlling the position of the cargo. However, this control is scenario-based and is specified by the user before model initialization only. They do not allow to change the position on demand in real-time. Thus, the capabilities of these systems may not always meet the demands of the task at hand. This reveals an important requirement for the modeling system—scalability. Some researchers' numerical models implement not only the lifting in the air but also the lifting off, splash zone crossing, submerging, and installation on the seabed [4, 8–10].

From this point of view, in this paper, the authors make a technical contribution to the development of an approach for analyzing the dynamic response of the offshore support vessel by using the widespread simulation environment MATLAB/Simulink and the MBD solver Simscape.

MATLAB/Simulink and Simscape are still not found extensive use as a platform for modeling crane vessels. The reason may be that Simulink is most often used to model complex mechanical systems such as robots and mechanisms. In addition, the hydrodynamic force calculation tool called WEC-Sim was developed relatively recently in MATLAB and is also dedicated to the analysis of wave energy converters with unchanging geometry.

The goal of this paper is to demonstrate a coupled CFD-MBD approach for modeling the dynamic response of a floating crane with real-time interactive control of crane elements. The advantage of the proposed approach is the use of the same software for both purposes—the determination of hydrodynamic forces and the determination of crane vessel motions as a multibody system. This increases the reliability of the simulation, and the use of the MATLAB environment makes the model very extensible. This will potentially make it possible to create a digital twin of an offshore crane vessel and introduce a real-time dynamic positioning system for its lifting equipment. A description of the observed problems associated with a real-time interactive simulation of offshore operations is presented. Simulation examples given include lifting, lowering, and handling operations with real-time interactive control by the operator. A comparison of the software used by other authors in related studies with the current paper is presented in Table 1.

Numerical procedure

Multibody dynamics

Offshore support vessel is a multibody system (Fig. 1), which the equation of motion in vector form is expressed as:

$$\begin{bmatrix} \mathbf{M} & \mathbf{C}_{\mathbf{x}}^{\mathrm{T}} \\ \mathbf{C}_{\mathbf{x}} & 0 \end{bmatrix} \begin{bmatrix} \ddot{\mathbf{x}} \\ \lambda \end{bmatrix} = \begin{bmatrix} \mathbf{F}_e \\ \gamma \end{bmatrix}, \tag{1}$$

where $\mathbf{M}$ is the mass and inertia matrix of the multibody system, $\ddot{\mathbf{x}}$ is acceleration vector; $\mathbf{F}_e$ and $\mathbf{C}_{\mathbf{x}}$ are vectors of external forces and constraint equations respectively; $\boldsymbol{\lambda}$ is the vector of Lagrange multipliers; $\boldsymbol{\gamma}$ is a vector that can

Table 1 The software used in the related studies

Study	Calculation and implementation of			
	Hydrodynamic coefficients	Hydrodynamic forces	MBD	Control
Cha et al. [2] and Hong et al. [3]	Commercial software	Developed by Cha et al. [5]	Developed by Cha et al. [5]	No
Viswanathan et al. [4]	OrcaFlex	OrcaFlex	OrcaFlex	SimulationX, slow computation
Jeong et al. [8]	Commercial software	Self-developed (Ha et al. [6])	Self-developed (Ha et al. [6])	Self-developed, scenario-based (pre-defined) control
Vorhölter et al. [10]	E4-ROLLS	E4-ROLLS	E4	E4, scenario-based (pre-defined) control
This paper	Capytaine	WEC-Sim (MATLAB)	MATLAB/Simscape	MATLAB/Simulink, real-time interactive control

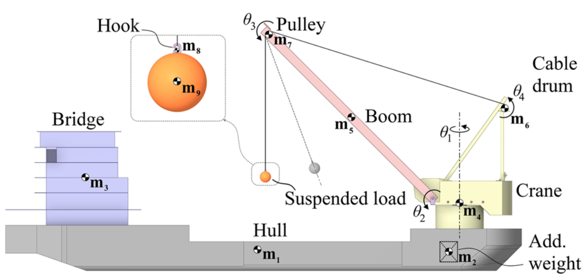

Fig. 1 General representation of a crane ship as a multibody system

be obtained by differentiating the constraint equations with respect to time twice:

$$\boldsymbol{\gamma} = \mathbf{C_x}\ddot{\mathbf{x}} \tag{2}$$

The origin of the coordinate system is located at the center of gravity of the vessel's hull (m_1 in Fig. 1). A specific form of the equation of motion for floating bodies was derived by Cummins [11], where external forces are represented as:

$$\mathbf{F}_e = \mathbf{F}_{hs} + \mathbf{F}_{exc} + \mathbf{F}_{rad} + \mathbf{F}_v + \mathbf{F}_{ext} \tag{3}$$

where $\mathbf{F}_{hs}$ is hydrostatic restoring force, $\mathbf{F}_{exc}$ is the wave excitation and diffraction force, $\mathbf{F}_{rad}$ is the force resulting from wave radiation, $\mathbf{F}_v$ is the viscous force, $\mathbf{F}_{ext}$ are other externally applied forces.

Thus, a significant part of the external forces acting on the floating multibody system is a complex of hydrodynamic forces. Integration of Eq. 1 is performed using the WEC-Sim software [12]. WEC-Sim is an open-source software developed in MATLAB/Simulink. It utilizes the multibody dynamics solver Simscape Multibody and makes it possible to build a model using its own block library in Simulink.

Calculation of hydrodynamic forces

In this paper, the hydrodynamic forces are calculated using the embedded algorithm of the WEC-Sim. The radiation term $\mathbf{F}_{rad}$ is calculated using the hydrodynamic coefficients of added mass $\mathbf{A}(\omega)$ and radiation damping $\mathbf{B}(\omega)$ depending on the incoming sea wave frequency ω.

These coefficients are pre-determined once using the open-source software Capytaine [13] by solving a boundary problem with governing equations according to the aforementioned potential flow theory. According to this theory, the flow velocity is a function of the flow velocity potential gradient:

$$\overrightarrow{v} = \nabla\phi(x, y, z) \tag{4}$$

where $\phi(x, y, z)$ is a scalar function called the flow velocity potential. The theory simplifies the flow to non-viscous and non-turbulent, but on the other hand, reduces the problem to the solution of a linear and rapidly computable Laplace equation.

Hydrodynamic coefficients $\mathbf{A}(\omega)$ and $\mathbf{B}(\omega)$ are dependent on the shape of submerged part and wave frequency ω and are calculated for each of the 6 degrees of freedom (DOF) of the floating body. A significant advantage of this CFD method is revealed here since in reality sea waves are irregular and the described approach allows to effectively calculate hydrodynamic forces for different sea states.

In case of sinusoidal steady-state response when the incoming wave is regular wave $\mathbf{F}_{rad}$ are calculated as follows:

$$\mathbf{F}_{rad}(t) = -\mathbf{A}(\omega)\ddot{\mathbf{x}} - \mathbf{B}(\omega)\dot{\mathbf{x}}, \tag{5}$$

where $\mathbf{A}(\omega)$ is added mass 6×6 matrix, $\mathbf{B}(\omega)$ is radiation damping 6×6 matrix, $\dot{\mathbf{x}}$ is velocity vector of floating body, and $\ddot{\mathbf{x}}$ is acceleration vector.

In linear case wave excitation forces $\mathbf{F}_{exc}$ are calculated only based on $\mathbf{F}_{exc}(\omega, \theta)$ coefficients obtained in the same way as the added mass and radiation damping, where θ is wave phase angle. But the necessary accuracy can be obtained by taking into account also the instantaneous body position and wave elevation. A similar problem consists in calculating the restoring forces $\mathbf{F}_{hs}$. In linear case $\mathbf{F}_{hs}$ are calculated depending on the instantaneous position (heave, roll, pitch, yaw) of the ship and a pre-computed 6×6 hydrostatic stiffness matrix containing $\mathbf{K}_{hs}$ coefficients. However, these coefficients will be valid only when the orientation of the crane parts is unchanged since changes in the orientation of the crane and the boom lead to the displacement of the center of gravity and the metacenter, and consequently the dynamics of the floating body. To handle this problem, an approach is used to calculate excitation (Froude–Krylov) and restoring forces on-the-fly by integrating the hydrostatic and the hydrodynamic pressures over the wetted surface of the body during each simulation time step [14].

In this paper, the free surface profile is modeled based on Airy (linear) wave theory for a given wave height, wave frequency, and water depth. The abovementioned pressures are calculated as follows:

$$p_{hs} = \rho g x_3, \tag{6}$$

$$p_{exc} = \frac{1}{2}\rho g h \frac{\cosh(k(z+d))}{\cosh(kd)}\cos\theta, \tag{7}$$

where ρ is water density, g is gravitational acceleration, x_3 is vertical displacement, h is wave height, k is wave number, z is vertical coordinate relative to the free surface, d is water depth, and θ is wave phase angle.

To circumvent the assumption of linear wave theory and predict kinematics for points above the mean water level, WEC-Sim uses a mathematical approach called Wheeler stretching [15]. Of course, there appear additional difficulties associated with ensuring the proper accuracy of the mesh. Also, the calculation time increases significantly, especially with a large number of diffracting elements.

To improve simulation accuracy and represent more or less realistic movement the viscous forces $\mathbf{F}_v$ were also included. Due to the essence of potential flow theory, these forces account for viscosity and turbulence of the flow not directly, but through damping coefficients:

$$\mathbf{F}_v(t) = -\mathbf{C}_v\dot{\mathbf{x}} - \mathbf{C}_D\dot{\mathbf{x}} \circ |\dot{\mathbf{x}}| \tag{8}$$

where $\mathbf{C}_v$ is the matrix of linear viscous damping coefficients, $\mathbf{C}_D$ is the matrix of quadratic drag coefficients.

These coefficients are different depending on the DOF and accordingly, matrices take the form of 6×6. They were determined using CFD simulations based on Navier–Stokes equations in separate solver considering the provisions of several regulatory documents [16, 17].

The abovementioned methods of accounting for nonlinear effects allow to overcome the disadvantages of the potential flow theory, preserving the advantage in the calculation speed. A schematic diagram of the overall calculation process is presented in Fig. 2, where $\boldsymbol{x}$, $\dot{\boldsymbol{x}}$ and $\ddot{\boldsymbol{x}}$ are the displacement, velocity, and acceleration vectors,

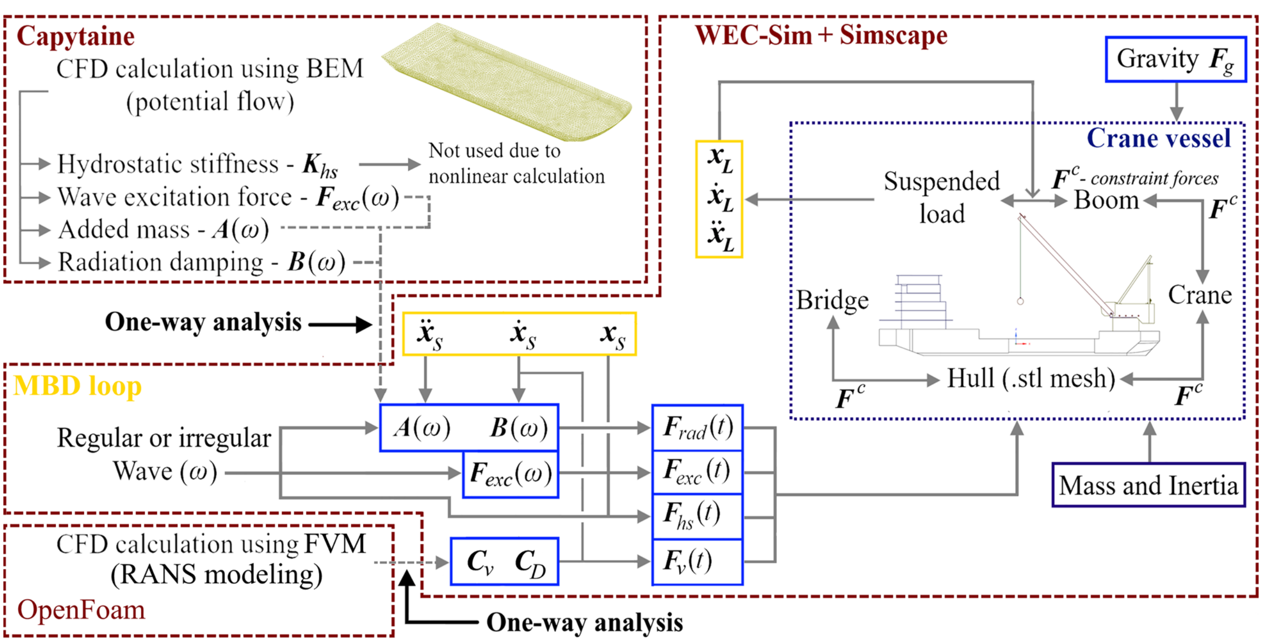

Fig. 2 Schematic diagram for calculating the dynamic response of a crane ship and suspended load

respectively. The subscripts S and L refer to the *ship* and the suspended *load* respectively. From the figure it can be seen that the CFD calculations in Capytaine are a kind of preparatory computation, which is performed once (one-way analysis). The forces are determined in the MBD loop itself through simple mathematical expressions using the hydrodynamic coefficients, mesh, and model input parameters.

Implementation

The model used in this paper is similar to the model in Fig. 1 presented earlier. It is the numerical analog of the model of the same size tested in reality in a laboratory wave basin. Different parts of the ship are represented as separate bodies, connected either rigidly or by revolute joints. On whole, the multibody system consists of 9 rigid bodies which motion in total is defined by 54 coordinates. Equation of motion (1) includes 44 algebraic constraints, so the system has 10 degrees of freedom. The length of the model is 1.77 m, total weight is 41.15 kg with a suspended mass of 0.16 kg. Inertia parameters are presented in Table 2. The gravitational forces acting on rigid bodies are considered as external forces $\mathbf{F}_{ext}$ in Eq. 1.

Experimental studies in the wave basin were conducted to verify the numerical model. During the experiment, the vessel was affected by a regular wave with a height of 0.02 m and a period of 1.4 s at a water depth of 0.16 m. As a result, recordings of vessel motions were obtained by capturing the position of special markers on the vessel using the motion capture system. The experimental setup is shown in Fig. 3.

To achieve high calculation accuracy, an STL model of 18540 elements was created. In the area of the wetted surface, the size of the elements was assumed to be smaller than above water. The calculated wave direction range included 360 directions with a 1-degree interval.

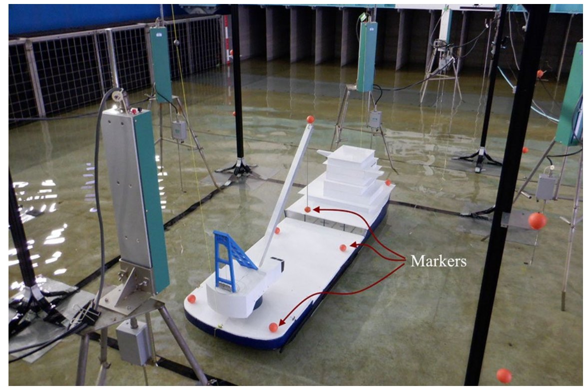

Fig. 3 Experimental setup for investigating the crane ship motions in a wave basin

The necessity of such precision is explained by the change of the incoming wave angle during the simulation process due to the rotation of the ship model. The radiation forces were determined from the local body-fixed coordinate system based upon the instantaneous relative yaw position of the body [18].

The calculated wave period range included 101 wave periods from 1 to 2 s, but in further MBD modeling a regular wave period of 1.4 s was used as in the laboratory experiment. To calculate linear and quadratic viscous damping coefficients ($\mathbf{C}_v$ and $\mathbf{C}_D$), decay tests and ship resistance RANS simulations were performed with the following flow parameters: flow velocity 0.05–0.3 m/s, Reynolds numbers from 8.09×10^4 to 4.85×10^5 The Volume of Fluid (VOF) method as a free-surface modeling technique was used to track gas-fluid interface.

The numerical model as a block diagram in the Simulink environment is shown in Fig. 4 and consists of both WEC-Sim blocks and fully compatible conventional Simscape blocks. As can be seen, the structural elements of

Table 2 Inertia parameters of the model

Body	Mass (kg)	Principal moments of inertia (kg m^2)			Center of gravity coordinates (m)		
		I_{p1}	I_{p2}	I_{p3}	x	y	z
Hull	21.4	0.541	5.580	6.052	0	0	0.015
Additional weight for balancing	9.76	0.044	0.007	0.043	0.656	0	0.010
Bridge	9.28	0.255	0.175	0.275	−0.622	−0.006	0.266
Crane	3.15	0.055	0.058	0.019	0.773	0.003	0.219
Boom	0.56	0.0001	0.033	0.033	0.313	0	0.483
Cable drum	0.001	8.424e−08	1.444e−07	1.678e−07	0.890	0	0.504
Pulley	0.001	5.140e−08	1.015e−07	5.143e−08	0.038	0	0.767
Hook	0	0	0	0	0.028	0	0.291
Suspended mass	0.16	2.310e−05	2.310e−05	2.310e−05	0.028	0	0.267

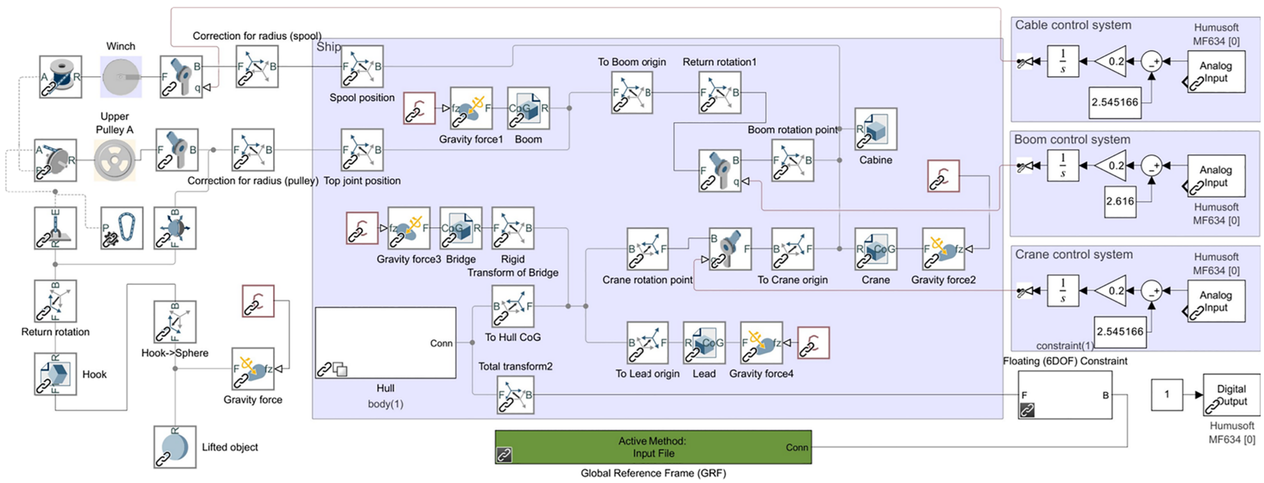

Fig. 4 Block diagram of the numerical model in Simulink environment

the vessel are represented by a set of solid body blocks and one WEC-Sim hydrodynamic body block. Additionally, the vessel is linked to the global reference frame. A set of blocks is connected to the frame of the top joint on the crane's boom, simulating the cable and suspended load. The cable is a massless, inextensible, and always taut cord, which is an assumption in this paper. To capture cable dynamics, e.g., accounting for vibrations, nonlinearity, and Karman vortex due to wind effects, improvement of this part is necessary, which is our future work. But it is sufficient for presenting the possibility of interactive cargo lifting.

Interactive control blocks that handle the analog input signal are connected to the joints representing the points of rotation of the structural elements (crane, boom, and cable drum). The analog devices transferring the input signal are 2-DOF manipulators connected to the workstation via an IO Board. Thus, the model described allows the simulation of a lifting operation with controlled crane and boom orientation and cable length.

The splash zone crossing and submerging stages are not considered in this paper. Today there are some solutions, mentioned earlier, which take into account the buoyancy force as a function of the submerged volume, e.g., in the paper of Jeong et al. [5]. However, this step requires a more detailed analysis, which one of the difficult and relevant problems in the application of the potential flow theory. The problem is that the submerged body is exposed not only to the buoyancy force but also to other natural forces (wind over water, sea waves, and currents). This fact raises the task of analyzing the load motions to a new level since it requires the real-time calculation of all its hydrodynamic coefficients.

Results and discussion

Non-interactive real-time simulation

This section presents the results of the simulation without any manual control of the crane parts. The amplitudes of the input signals are zero. Therefore, the crane cabin, boom, and cable length remained fixed throughout the simulation. The purpose of this step is to verify the numerical model by comparing the simulation results with the experiments.

Figure 5 shows the comparison of heave and pitch motions and horizontal (along the ship's longitudinal axis) motions of the load suspended on 0.5 m cable. The results illustrate that the numerical model gives the necessary accuracy of calculations. The maximum errors between experiment and simulation with respect to the maximum amplitude were: 4.3% for Heave, 6.9% for Pitch, and 5% for suspended load x motions.

Moreover, the time of calculation of 30 s case was about 20 s with time step 0.005 s, i.e., it is faster than real-time. The calculations were performed on an Intel Core i9-12900K processor having 16 cores.

Interactive real-time simulation

At this stage, the crane and the ship's boom were controlled interactively by the operator (Fig. 6). The first simulations with the ode4 solver did not achieve calculation convergence at the selected time step of the same constant size. If the position of the crane elements changed too quickly, the computing slowed down a lot and increased again when the position remained static. Therefore, we decided to use the ode45 solver with a variable time step. After switching to this solver, the convergence problem was eliminated.

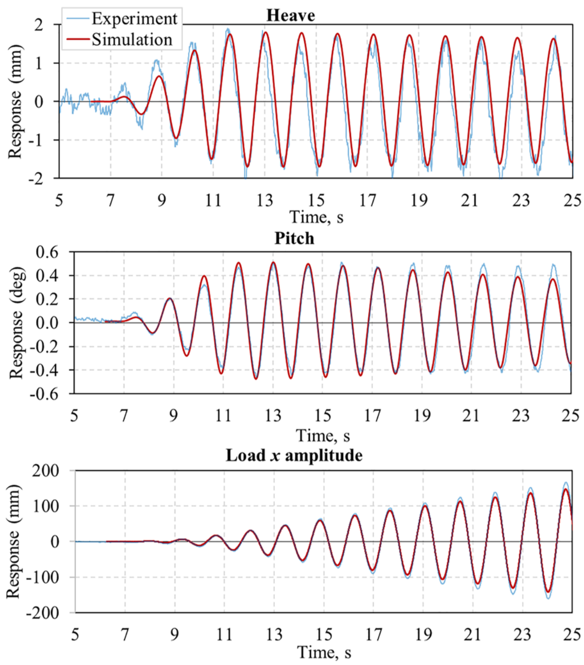

Fig. 5 Comparison of model motions in simulation and experiment

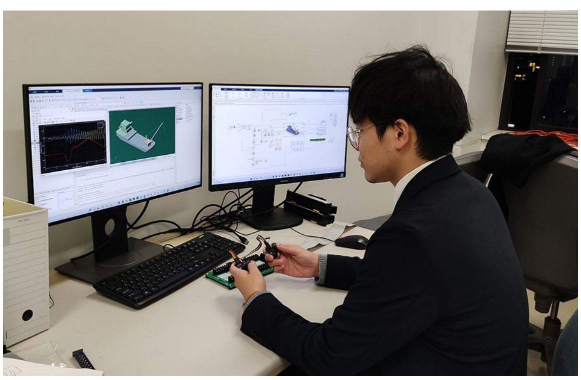

Fig. 6 Interactive control of the model by the operator during the simulation

In the simulated case, the change of position of the ship's parts occurred sequentially. The response of the vessel in the simulated situation is shown in Fig. 7. From a neutral position at 1.3 s (time moment 1), the ship's crane began to rotate and was eventually rotated by 95.9 degrees (time moment 2). Due to the change in position of the centers of gravity of the crane, boom, and suspended load, an additional roll of the vessel occurred. The model reached a new neutral position, as determined by a non-linear calculation of the restoring forces. Then, at simulation time 9 s, the crane boom was moved, which also resulted in inverse rolling (time moment 3). At the time moment 4, the crane's boom changed its position again. The displacement of the boom center of gravity from the vessel's longitudinal axis resulted in a progressive yawing of the vessel. Therefore, interpolation of the hydrodynamic coefficients is important, even if there is no manual control of the vessel's rotation (e.g., control of engines).

Another interesting result is the time step variation during the computation process. Figure 8 shows the distribution of the time step size during the simulation. It can be seen that a significant part of the computation was performed with a timestep size from 5.7×10^{-4} s to 1.6×10^{-3} s. Hence, the solver sometimes automatically reduced the time step in order to resolve the complexity of the problem.

The total number of calculation steps of the 30 s event was 12,203, which is significantly more than 6000 steps when using the ode4 solver with a fixed time step in the previous stage without interactive control. During the simulation, there were some missed ticks due to the complexity of the model. This can easily be fixed, for instance, by using a simpler ship hull mesh. The total elapsed time in the case of the interactive crane control turned out to be 24.9 s, which leads to a ratio of model time/elapsed time equal to 1.2 when using a conventional PC.

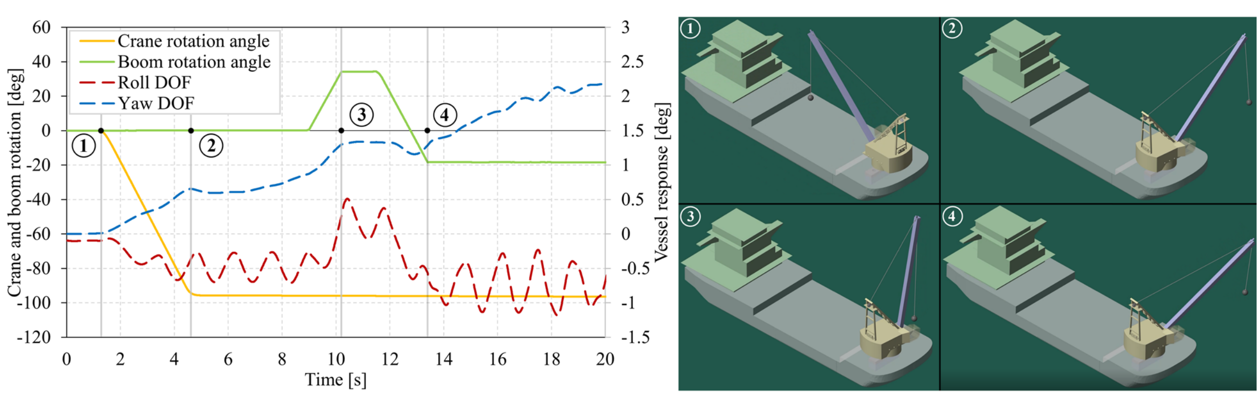

Fig. 7 The dynamic response of the crane ship model during the interactive control process

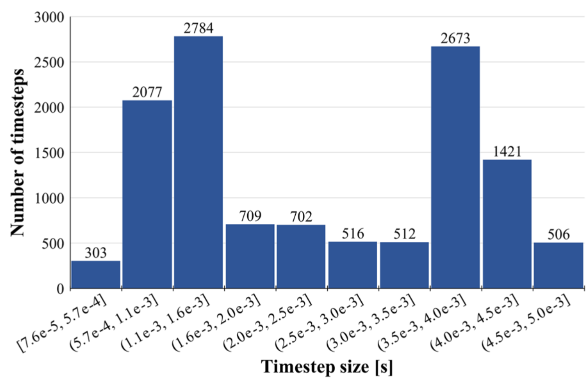

Fig. 8 Distribution of the time step value during the simulation

Hence, the presented numerical model in MATLAB Simulink provides interactive control of model elements preserving real-time computing and having sufficient calculation accuracy of the floating vessel dynamics. Although there are some problems with synchronization, these can be successfully solved due to the scalability of the model.

Conclusion and future works

In summary, the following conclusions can be drawn.

Firstly, hydrodynamics based on potential flow theory provides the necessary accuracy to solve the given engineering problem. At the same time, the possibility to consider multiple sea states is an indisputable advantage and one of the necessary components in the creation of digital twins of crane ships.

Secondly, this paper shows an approach to creating an interactive model that is both computationally fast and scalable for different tasks. The latter is achieved by using the powerful mathematical tool Simulink for both tasks—calculation of hydrodynamic forces and motions of ship elements. In this case, the extensibility of the model is limited only by the skills of the developers and the available computational resources.

Of course, the proposed model has some limitations. Thus, the theory of potential flow gives large errors, where high wave nonlinearity can occur and significant vortex effects can appear. Accordingly, the dynamics of the vessel and, as a consequence, the dynamics of the cargo cannot be accurately predicted in this case. Nevertheless, the area of application of the proposed solution is the dynamic analysis of the vessel during marine operations, where the sea conditions are not so severe and can be successfully described using the proposed approach.

The scalability of the model will be introduced by the authors in future works, among which it is planned to consider the cargo-deck collision to implement lifting-up and cargo installation operations. Another direction of extension of the approach is to consider the influence of wind and currents, both on the ship itself and the suspended load. This is currently possible using third-party libraries through API interfaces but will be addressed by incorporating additional algorithms and blocks into the model. We also plan to conduct an enhanced experiment in a wave basin with manual control of crane parts for additional validation of the method.

The methods under development have the potential to find widespread application in decreasing the sway of suspended loads to ensure safe and highly accurate offshore crane operations.

Acknowledgements
We express our gratitude to the scientific team of Naruo Research Center for technical support and for providing the data on experiments in the wave basin.

Author contributions
OM developed the numerical model of the floating crane vessel, conducted numerical analysis, and drafted the work. HY developed and analyzed the control part and lift-up operation elements of the numerical model, and revised the paper. TH made the main contributions to the conception and design of the work, interpretation of data, and paper revision.

Funding
Not applicable.

Availability of data and materials
Not applicable.

Declarations

Competing interests
The authors declare that they have no competing interests.

Received: 14 March 2023 Accepted: 10 July 2023
Published online: 26 July 2023

References

1. Wang Y, Tang Z, Wang L, Wang X (2022) Linear and quadratic damping coefficients of a single module of a very large floating structure over variable bathymetry: physical and numerical free-decay experiments. J Ocean Eng Sci 7(6):607–618. https://doi.org/10.1016/j.joes.2021.10.011
2. Cha J-H, Roh M-I, Lee K-Y (2010) Dynamic response simulation of a heavy cargo suspended by a floating crane based on multibody system dynamics. Ocean Eng 37(14–15):1273–1291. https://doi.org/10.1016/j.oceaneng.2010.06.008
3. Hong J-W, Roh M-I, Ham S-H, Ha S (2016) Dynamic simulation of subsea equipment installation using an offshore support vessel based on flexible multibody system dynamics. J Mar Sci Technol 24(4):15. https://doi.org/10.6119/JMST-016-0323-1
4. Viswanathan S, Satheesh Babu PK, Holden C, Egeland O (2021) A Co-simulation Methodology for Offshore Load Handling. In: Proceedings of the International Conference on Advances in Naval and Ocean Engineering (iCANOE '21)
5. Cha J-H, Roh M-I, Lee K-Y (2010) Integrated simulation framework for the process planning of ships and offshore structures. Robot Comput Integr Manuf 26(5):430–453. https://doi.org/10.1016/j.rcim.2010.01.001
6. Ha S, Ku N-K, Roh M-I, Hwang H-J (2015) Multibody system dynamics simulator for process simulation of ships and offshore plants in shipyards. Adv Eng Softw 85:12–25. https://doi.org/10.1016/j.advengsoft.2015.02.008

7. Ku N, Ha S (2014) Dynamic response analysis of heavy load lifting operation in shipyard using multi-cranes. Ocean Eng 83:63–75. https://doi.org/10.1016/j.oceaneng.2014.03.026
8. Jeong D-H, Roh M-I, Ham S-H (2016) Lifting simulation of an offshore supply vessel considering various operating conditions. Adv Mech Eng 8(6):1–13. https://doi.org/10.1177/1687814016654633
9. Nam BW, Hong SY, Kim YS, Kim JW (2015) Integrated simulations of a floating crane installation vessel with DP systems in waves. J Adv Res Ocean Eng 1(2):85–93. https://doi.org/10.5574/JAROE.2015.1.2.085
10. Vorhölter H, Hatecke H and Feder D-F (2015) Design study of floating crane vessels for lifting operations in the offshore wind industry. In: Proceedings of International marine design conference, The University of Tokyo, Tokyo, 11–14 May 2015
11. Cummins WE (1962) The impulse response function and ship motions. Schiffstechnik 9:101–109
12. WEC-Sim (Wave Energy Converter SIMulator) – WEC-Sim documentation, https://WEC-Sim.github.io/WEC-Sim/master/index.html. Accessed 26 Oct 2022
13. Ancellin M, Dias F (2019) Capytaine: a Python-based linear potential flow solver. J Open Source Softw 4(36):1341. https://doi.org/10.21105/joss.01341
14. Lawson M, Yu Y-H, Nelessen A, Ruehl K and Michelen C (2014) Implementing Nonlinear Buoyancy and Excitation Forces in the WEC-Sim Wave Energy Converter Modeling Tool. In: Proceedings of 33rd International Conference on Ocean, Offshore and Arctic Engineering, San Francisco, California, 8–13 June 2014. https://doi.org/10.1115/OMAE2014-24445
15. Wheeler JD (1970) Method for calculating forces produced by irregular waves. J Petrol Technol 22(3):359–367. https://doi.org/10.2118/2712-PA
16. ITTC – Recommended Procedures and Guidelines (2014) 7.5-03-02-03 Practical Guidelines for Ship CFD Applications
17. ITTC – Recommended Procedures and Guidelines (2014) 7.5-03-02-04 Practical Guidelines for Ship CFD Applications
18. Forbush D, Ruehl K, Ogden D, van Rij J, Yu Y, Tom N (2020) Development and validation of passive yaw in the opensource WEC-Sim code. In: Proceedings of the 39th International Conference on Ocean, Offshore, and Arctic Engineering, 3–7 August 2020

Publisher's Note